Thermochimica Acta, 234 (1994) 201–219
Elsevier Science B.V., Amsterdam
SSDI 0040-6031(93)01504-V

Thermal degradation and crystallographic data of metal complexes of oxopurines and thiopurines [1]

Erich Dubler * and Gaby Hänggi

Institute of Inorganic Chemistry, University of Zürich, Winterthurerstrasse 190, CH-8057 Zürich (Switzerland)

(Received 18 December 1992; accepted 4 March 1993)

Abstract

The thermal behaviour of metal compounds of the naturally occurring oxopurines hypoxanthine, xanthine and uric acid and of the synthetic pyrazolopyrimidines allopurinol and alloxanthine as well as of the thiopurine 6-mercaptopurine has been investigated using thermogravimetric and X-ray crystallographic techniques. The thermogravimetric data confirm the structural characteristics of the metal complexes. The degradation of hydrated complexes occurs in two steps with a dehydration reaction followed by complete decomposition to the corresponding metal oxides. Anhydrous compounds are decomposed in one step overall reactions. The temperature range of dehydrations of the hydrated complexes strongly depends on the binding mode of the water molecules. The reaction rate of the final decompositions of these complexes seems to be influenced by the respective metal ions. Copper and iron complexes show a sharp increase in the reaction rate in respect of the complexes of cobalt and nickel, whereas zinc, cadmium and manganese compounds are slowly decomposed over a wide temperature range.

INTRODUCTION

The oxopurines hypoxanthine and xanthine are of biological importance, since they are metabolic intermediate products of purine metabolism. Hypoxanthine (1,7-dihydro-6H-purin-6-one), formed by degradation of nucleic acids, is oxidized by the molybdenum- and iron-containing enzyme xanthine oxidase via xanthine to uric acid, which subsequently is released from the active site of the enzyme [1]. Disturbances in purine metabolism result in an increase of the uric acid level and in the deposition of sodium hydrogenurate monohydrate crystals in joints. This disease, known as gout, is clinically treated by the drug allopurinol (pyrazolo[3,4-d]pyrimidin-6-one), which is also a substrate for xanthine oxidase [2]. Alloxanthine (pyrazolo[3,4-d]pyrimidin-2,6-dione), the enzymatic oxidation product of the drug allopurinol, inactivates xanthine oxidase by irreversible coordination to the reduced form of the molybdenum centre of the enzyme [3].

* Corresponding author.
[1] Dedicated to Hans Georg Wiedemann.

Therefore, the formation of uric acid is inhibited, and patients receiving the drug allopurinol excrete much of their purines as hypoxanthine and xanthine.

The synthetic purine derivative 6-mercaptopurine (MP) is a drug used worldwide for the treatment of human leukaemia. In the anabolic mechanism of action of this agent, MP is converted within the cell to the respective ribonucleotide, which inhibits the purine biosynthesis [4]. Today, about 80% of the children suffering from leukaemia show complete remission after administration of MP in combination with other chemotherapeutic agents. In the catabolic reaction, MP is oxidized to inactive thiouric acid. This reaction is also catalyzed by xanthine oxidase [5]. Synthesis and reactivity screenings of metal complexes of active molecules such as MP have been performed in order to achieve an enhanced therapeutic effect in combination with decreased toxicity. It has been found that platinum or palladium complexes of MP show enhanced activity with respect to the free ligand [6]. In addition, metal complexes of MP are of importance in view of their function as repository, slow-release or long-acting prodrugs for MP. In this context, synthesis, thermogravimetric characterization and crystal structure analysis of metal complexes of the purine derivatives mentioned above and shown in Fig. 1 have been performed.

EXPERIMENTAL

Materials

Hypoxanthine, xanthine, uric acid and 6-mercaptopurine monohydrate were obtained from Fluka, Buchs, Switzerland and used without further purification. Allopurinol was purchased from Sigma Chemical Co., Bâle,

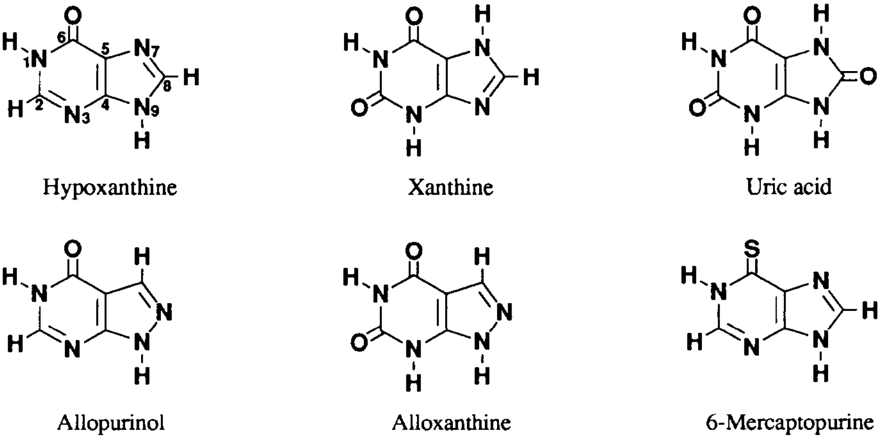

Fig. 1. Purine derivatives.

Switzerland, whereas alloxanthine was prepared according to a method previously reported [7]. The metal salts, of analytical reagent grade, were obtained from Fluka, Buchs, Switzerland.

Syntheses

Complexes of hypoxanthine have been synthesized in the form of single crystals from diluted sulphuric acid containing the respective metal sulphates. The reaction of metal chlorides with xanthine in hydrochloric acid resulted in the formation of xanthine compounds. Another complex of xanthine has been prepared from aqueous solution using copper nitrate as inorganic salt. Single crystals of allopurinol complexes have been obtained from aqueous solutions of the ligand by addition of an excess of the corresponding metal sulphates or chlorides. Alloxanthine complexes were obtained by treating an excess of the corresponding metal nitrate or chloride with a hot aqueous solution of the ligand. The reaction of 6-mercaptopurine with metal chlorides in dilute hydrochloric acid has resulted in the formation of metal complexes of 6-mercaptopurine with different structure types. Hydrogenurate compounds have been crystallized from aqueous solutions or from TMS-gels containing K(hydrogenurate$^-$) and the respective metal chloride. Detailed descriptions of the syntheses have been given elsewhere [7–9]. The stoichiometry of these compounds was derived from chemical analyses and thermogravimetric investigations.

Thermogravimetric data

The thermogravimetric data were collected on instruments of the type TGS-2 or TAS-7 (Perkin-Elmer) and TA-2000 (Mettler) under flowing oxygen or nitrogen atmosphere or in static air. Heating rates were 5–10°C min^{-1} in the temperature range from room temperature to 600–800°C. Sample masses used were 1–20 mg. Evolved gas analyses were simultaneously performed with a Balzers QMG-511 quadrupole mass spectrometer coupled to the thermobalance.

X-Ray crystallography

Cell parameters of single crystals were obtained from least-squares refinements on an Enraf-Nonius CAD-4 diffractometer. The structures of most compounds described in this paper have been determined by single crystal X-ray diffraction analysis. Stoichiometries, crystallographic data and structural formulae of all compounds investigated are summarized in Tables 1–3 respectively.

The final products of the thermal degradations were identified by X-ray powder diffraction diagrams produced on a Nonius Guinier IV camera

TABLE 1

Structural data for metal complexes of hypoxanthine, xanthine, allopurinol and alloxanthine

Compound	$V_{calc}/Å^3$	Z	Space group	Structural formula	Coordination	Ref.
Co(hypoxanthine)$SO_4 \cdot 5H_2O$	648.4(3)	2	$P\bar{1}$	[Co(hypoxanthine)$(H_2O)_5$]SO_4	N(7)	14
Ni(hypoxanthine)$SO_4 \cdot 5H_2O$	640.4(3)	2	$P\bar{1}$	[Ni(hypoxanthine)$(H_2O)_5$]SO_4	N(7)	15
Cu(hypoxanthine)$SO_4 \cdot 2H_2O$	489.5(7)	2	$P\bar{1}$	[Cu_2(μ-hypoxanthine)$_2(SO_4)_2(\mu$-$H_2O)_2(H_2O)_2$]	N(3)/N(9)	16
Co(hypoxanthine)$SO_4 \cdot 2H_2O$	496.7(5)	2	$P\bar{1}$	[Co_2(μ-hypoxanthine)$_2(SO_4)_2(\mu$-$H_2O)_2(H_2O)_2$]	N(3)/N(9)	17
Zn(hypoxanthine)$SO_4 \cdot 2H_2O$	497.1(3)	2	$P\bar{1}$	[Zn_2(μ-hypoxanthine)$_2(SO_4)_2(\mu$-$H_2O)_2(H_2O)_2$]	N(3)/N(9)	16
Cd(hypoxanthine)$SO_4 \cdot 2H_2O$	523.9 (4)	2	$P\bar{1}$	[Cd_2(μ-hypoxanthine)$_2(SO_4)_2(\mu$-$H_2O)_2(H_2O)_2$]	N(3)/N(9)	16
Cu(hypoxanthine)$SO_4 \cdot H_2O$	464.3(3)	2	$P2_1$	Poly[Cu(μ-hypoxanthine)(μ-SO_4)H_2O]	N(3)/N(7)	14
Cu(xanthine)$_2(NO_3)_2 \cdot 2H_2O$	428.6(3)	1	$P\bar{1}$	[Cu(xanthine)$_2(NO_3)_2(H_2O)_2$]	N(9)	18
Cu(xanthine)$_2Cl_2 \cdot 2H_2O$	430.3(7)	1	$P\bar{1}$	[Cu(xanthine)$_2Cl_2$] $\cdot 2H_2O$	N(9)	18
Zn(xanthine)$_2Cl_2$	1508.6(3)	4	$C2/c$	[Zn(xanthine)$_2Cl_2$]	N(9)	18
(xanthine$^+$)$_2$[$ZnCl_4$]	857.3(7)	2	$Pmn2_1$	(xanthine$^+$)$_2$[$ZnCl_4$]		19
Cu(allopurinol)$_2SO_4 \cdot 4H_2O$	875.7(10)	2	$P\bar{1}$	[Cu(allopurinol)$_2SO_4(H_2O)_3$] $\cdot H_2O$	N(8)	20
Co(allopurinol)$_2SO_4 \cdot 4H_2O$	881.8(5)	2	$P\bar{1}$	[Co(allopurinol)$_2SO_4(H_2O)_3$] $\cdot H_2O$	N(8)	21
Ni(allopurinol)$_2SO_4 \cdot 4H_2O$	872.6(8)	2	$P\bar{1}$	[Ni(allopurinol)$_2SO_4(H_2O)_3$] $\cdot H_2O$	N(8)	21
Zn(allopurinol)$_2SO_4 \cdot 4H_2O$	883.2(8)	2	$P\bar{1}$	[Zn(allopurinol)$_2SO_4(H_2O)_3$] $\cdot H_2O$	N(8)	21
Cd(allopurinol)$_2SO_4 \cdot 4H_2O$	918.0(10)	2	$P\bar{1}$	[Cd(allopurinol)$_2SO_4(H_2O)_3$] $\cdot H_2O$	N(8)	21
Co(allopurinol)$_2Cl_2 \cdot 2H_2O$	369.8(3)	1	$P\bar{1}$	[Co(allopurinol)$_2Cl_2(H_2O)_2$]	N(8)	22
Ni(allopurinol)$_2Cl_2 \cdot 2H_2O$	363.8(7)	1	$P\bar{1}$	[Ni(allopurinol)$_2Cl_2(H_2O)_2$]	N(8)	22
Zn(allopurinol$^-$)Cl $\cdot H_2O$	394.1(3)	2	$P\bar{1}$	[Zn_2(μ-allopurinol$^-$)$_2Cl_2(H_2O)_2$]	N(8)/N(9)	23
Cu(alloxanthine)$_2(NO_3)_2 \cdot 2H_2O$	429.6(7)	1	$P\bar{1}$	[Cu(alloxanthine)$_2(NO_3)_2(H_2O)_2$]	N(9(	24
Co(alloxanthine)$_2(NO_3)_2 \cdot 2H_2O$	434.8(6)	1	$P\bar{1}$	[Co(alloxanthine)$_2(NO_3)_2(H_2O)_2$]	N(9)	24
Zn(alloxanthine)$_2Cl_2$	1470.6(12)	4	$Pbcn$	[Zn(alloxanthine)$_2Cl_2$]	N(9)	24

TABLE 2

Structural data for hydrogenurate compounds

Compound	V_{calc}/Å^3	Z	Space group	Structural formula	Coordination	Ref.
Na(hydrogenurate$^-$) · H_2O	355.7	2	$P\bar{1}$		O(2), O(6), O(8)	9
NH_4(hydorgenurate$^-$)	1235 [a]	8				9
K(hydrogenurate$^-$)						9
Rb(hydrogenurate$^-$)						9
Mg(hydrogenurate$^-$)$_2$ · $8H_2O$ (phase I)	982.4(6)	2	$P2_1/c$	[Mg(H_2O)$_6$](hydrogenurate$^-$)$_2$ · $2H_2O$		12
Mg(hydrogenurate$^-$)$_2$ · $8H_2O$ (phase II)	968.8(6)	2	$P2_1/c$	[Mg(H_2O)$_6$](hydrogenurate$^-$)$_2$ · $2H_2O$		12
Ca(hydrogenurate$^-$)$_2$ · $6H_2O$	901.9	2				9
Co(hydrogenurate$^-$)$_2$ · $6H_2O$	1611.9	4				9
Cu(hydrogenurate$^-$)$_2$ · $6H_2O$	1793.9	4	$P2_1/n$	[Cu(hydrogenurate$^-$)$_2$(H_2O)$_3$] · $3H_2O$	N(9)	9

[a] The cell parameters were determined by powder X-ray diffractometry.

TABLE 3

Structural data for metal complexes of mercaptopurine

Compound	$V_{calc}/Å^3$	Z	Space group	Structural formula	Coordination	Ref.
Mn(mercaptopurine)$_2$Cl$_2$ · CH$_3$OH	897.2(6)	2	$P\bar{1}$	[Mn(mercaptopurine)$_2$Cl$_2$]	N(7)	8
Co(mercaptopurine)$_2$Cl$_2$ · CH$_3$OH		2	$P\bar{1}$	[Co(mercaptopurine)$_2$Cl$_2$]	N(7)	8
Zn(mercaptopurine)$_2$Cl$_2$ · CH$_3$OH	886.5(6)	2	$P\bar{1}$	[Zn(mercaptopurine)$_2$Cl$_2$]	N(7)	8
Fe(mercaptopurine)$_2$Cl$_2$ · CH$_3$OH		2	$P\bar{1}$	[Fe(mercaptopurine)$_2$Cl$_2$]	N(7)	8
Cd(mercaptopurine)$_4$Cl$_2$	685.9(6)	1	$P\bar{1}$	[Cd(mercaptopurine)$_2$Cl$_2$] (mercaptopurine)$_2$	N(7)/S	13
Fe(mercaptopurine)$_4$Cl$_2$	672.6(8)	1	$P\bar{1}$	[Fe(mercaptopurine)$_2$Cl$_2$] (mercaptopurine)$_2$	N(7)/S	8
Co(mercaptopurine)$_4$Cl$_2$	671.8(6)	1	$P\bar{1}$	[Co(mercaptopurine)$_2$Cl$_2$] (mercaptopurine)$_2$	N(7)/S	8
Pt(mercaptopurine$^-$)$_2$ · 2H$_2$O	714.5(4)	2	$P2_{1/c}$	[Pt(mercaptopurine$^-$)$_2$] · 2H$_2$O	N(7)/S	8
Fe$_2$(mercaptopurine)$_3$Cl$_5$	1379.7(9)	2	$P6_3$	[Fe(mercaptopurine)$_3$]$^{2+}$ [FeCl$_4$]$^-$ Cl$^-$	N(7)/S	8
Cu(mercaptopurine$^+$)Cl$_2$	437.5(12)	2	$P\bar{1}$	[Cu$_2$(mercaptopurine$^+$)$_2$(μ-Cl)$_2$Cl$_2$]	S	13
Cd(mercaptopurine$^-$)$_2$ · 2H$_2$O	369.7(4)	1	$P\bar{1}$	Poly[Cd(μ-mercaptopurine$^-$)$_2$] · 2H$_2$O	N(7)/S	13
Cd$_3$(mercaptopurine)$_4$Cl$_6$	841.5(8)	1	$P\bar{1}$	Poly[Cd$_2$(μ-mercaptopurine)$_2$Cl$_4$] and [Cd(mercaptopurine)$_2$Cl$_2$]	N(7)/S	8

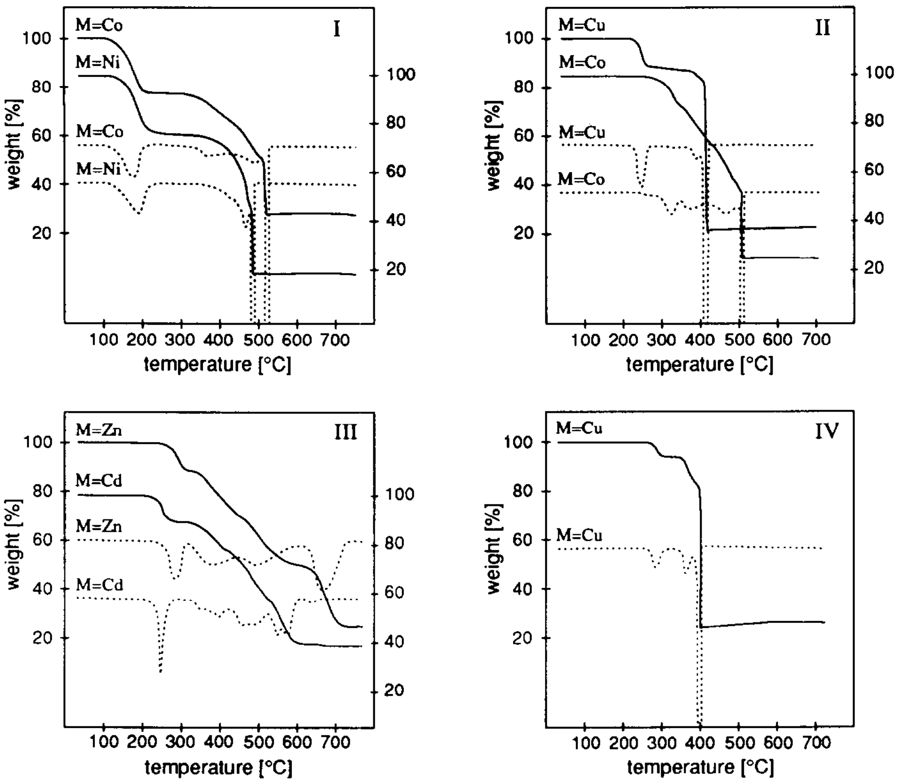

Fig. 2. Thermogravimetric (solid lines) and differential thermogravimetric (dotted lines) curves of the thermal degradation of metal hypoxanthine complexes in flowing oxygen atmosphere: I, M(hypoxanthine)$SO_4 \cdot 5H_2O$ (M is Co, Ni); II, M(hypoxanthine)$SO_4 \cdot 2H_2O$ (M is Cu, Co); III, M(hypoxanthine)$SO_4 \cdot 2H_2O$ (M is Zn, Cd); IV, Cu-(hypoxanthine)$SO_4 \cdot H_2O$.

using Cu $K\alpha_1$ or Fe $K\alpha_1$ radiation. The diffraction data were verified using the JCPDS powder diffraction file [10].

RESULTS AND DISCUSSION

Hypoxanthine (hyxan)

The thermal degradation data are presented in Fig. 2 and Table 4. Metal complexes of hypoxanthine exhibit a strikingly uniform decomposition behaviour including a dehydration reaction followed by complete decomposition to the corresponding metal oxides. The temperature ranges of the dehydration processes show a strong relationship to the binding mode of the water molecules of the respective metal complex. The elimination of the five coordinating water molecules of monomeric complexes of the type M(hyxan)$SO_4 \cdot 5H_2O$ (M is Co, Ni) occurs in a one step process resulting in a relatively stable dehydrated phase. The dimeric complexes

TABLE 4

Thermal degradation [a] of metal hypoxanthine complexes

Complex	Dehydration			Total decomp.		Final product
	Mass loss/%		T/°C	Mass loss/%	T/°C	
$Co(hyxan)SO_4 \cdot 5H_2O$	$-5H_2O$	23.6 (c) 23.7 (o)	100–220	78.9 (c) 76.5 (o)	320–520	Co_3O_4
$Ni(hyxan)SO_4 \cdot 5H_2O$	$-5H_2O$	23.6 (c) 23.7 (o)	110–250	80.4 (c) 80.2 (o)	300–490	NiO
$Cu(hyxan)SO_4 \cdot 2H_2O$	$-2H_2O$	10.9 (c) 11.0 (o)	210–260	76.0 (c) 76.1 (o)	270–420	CuO
$Co(hyxan)SO_4 \cdot 2H_2O$	$-2H_2O$	11.0 (c) 11.9 (o)	230–340	75.5 (c) 76.0 (o)	340–500	Co_3O_4
$Zn(hyxan)SO_4 \cdot 2H_2O$	$-2H_2O$	10.8 (c) 10.8 (o)	200–320	75.6 (c) 75.1 (o)	320–720	ZnO
$Cd(hyxan)SO_4 \cdot 2H_2O$	$-2H_2O$	9.5 (c) 9.8 (o)	180–270	 60.8 (o)	310–660	$CdO/Cd_3O_2SO_4$
$Cu(hyxan)SO_4 \cdot H_2O$	$-1H_2O$	5.7 (c) 6.0 (o)	270–300	74.6 (c) 73.7 (o)	340–400	CuO

[a] c, Calculated; o, observed.

$M(hyxan)SO_4 \cdot 2H_2O$ (M is Cu, Co, Zn, Cd) involving bridging and terminal water molecules are also dehydrated in one step reactions, but starting at markedly higher temperatures than the dehydration of the monomeric complexes. Finally, the polymeric copper complex $Cu(hyxan)SO_4 \cdot H_2O$ shows enhanced thermal stability, and the elimination of the coordinating water molecule is observed at even higher temperatures (270–300°C).

The subsequent decomposition to the respective metal oxides occurs in several overlapping steps indicating a complicated reaction mechanism. Generally the pyrolysis of copper complexes shows a higher reaction rate than that of the cobalt and nickel compounds, probably due to the catalytic role of the copper ions. Complexes of zinc and cadmium, in contrast, exhibit slow pryolysis over a wide temperature range.

Xanthine (xan)

The thermal degradation data are presented in Fig. 3 and Table 5. The thermogravimetric curve of $Cu(xan)_2(NO_3)_2 \cdot 2H_2O$ shows two well resolved steps. The first mass loss corresponds to the simultaneous elimination of the two coordinating water molecules and of the two nitrate groups, probably in the form of HNO_3. The intermediate product is decomposed with a sharp increase in the reaction rate at a temperature of 360°C to the final residue CuO.

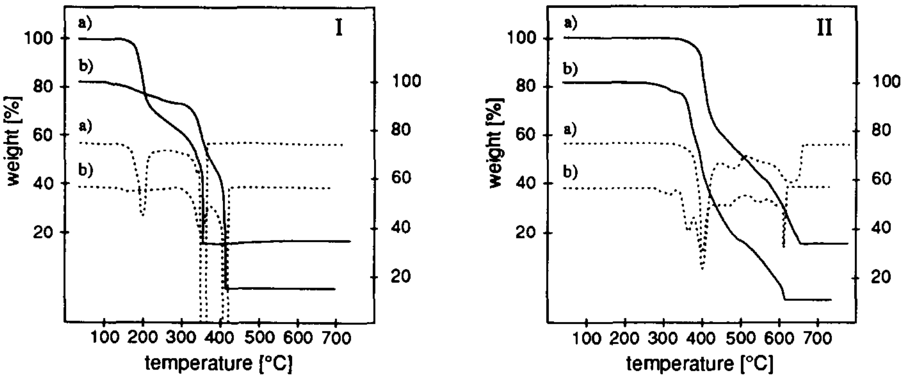

Fig. 3. Thermogravimetric (solid lines) and differential thermogravimetric (dotted lines) curves of the thermal degradation of metal xanthine complexes in flowing oxygen atmosphere: I (a) $Cu(xanthine)_2(NO_3)_2 \cdot 2H_2O$, (b) $Cu(xanthine)_2Cl_2 \cdot 2H_2O$; II, (a) $Zn(xanthine)_2Cl_2$, (b) $(xanthine^+)_2[ZnCl_4]$.

The thermal decomposition of $Cu(xan)_2Cl_2 \cdot 2H_2O$ takes place in three steps. The first step can be attributed to the emission of the inserted water molecules. The decrease in mass of the first step of about 9.2% is higher than expected for two water molecules (7.6%). The assumption of a variable water content, averaging from two to three water molecules per formula unit, is supported by the observed density of 1.90 g cm^{-3}, which corresponds to the composition $Cu(xan)_2Cl_2 \cdot 3H_2O$ (calculated value 1.90 g cm^{-3}). Since in the structural analysis, two water molecules only could be localized, and in agreement with the analytical data we report here two water molecules of hydration. The further degradation of the

TABLE 5

Thermal degradation [a] of metal xanthine complexes

Compound	Dehydration			Total decomp.		Final product
	Mass loss/%		T/°C	Mass loss/%	T/°C	
$Cu(xan)_2(NO_3)_2 \cdot 2H_2O$	$-2H_2O$	6.8 (c)	130–220	84.9 (c_{CuO})	220–360	CuO/Cu_2O
	$-2HNO_3$	23.9 (c)		84.1 (o)		
		28.5 (o)				
$Cu(xan)_2Cl_2 \cdot 2H_2O$	$-2H_2O$	7.6 (c)	70–290	83.2 (c)	290–420	CuO
		9.2 (o)		84.8 (o)		
$Zn(xan)_2Cl_2$				81.5 (c)	320–660	ZnO
				85.6 (o)		
$(Xan^+)_2[ZnCl_4]$		3.8 (o)	200–320	84.1 (c)	320–610	ZnO
				89.6 (o)		

[a] c, Calculated; o, observed.

anhydrous complex to CuO occurs in two overlapping dehalogenation and decomposition reactions respectively and finishes at about 420°C.

The thermal analysis of anhydrous $Zn(xan)_2Cl_2$ shows that the complex is thermally stable under the experimental conditions used up to a temperature of 320°C. The subsequent degradation to the final residue ZnO occurs in two steps with the formation of an unstable intermediate product due to the overlapping of dehalogenation and pyrolysis reactions.

The thermal behaviour of $(xan^+)_2[ZnCl_4]$ in flowing oxygen atmosphere is very similar to that described for the degradation of this compound in static air or nitrogen atmosphere [11] with the exception of a mass loss of 3.8% which could be attributed to the elimination of adsorbed water. The crystal structure determination of this compound, however, excludes the existence of a water molecule of hydration. The subsequent decomposition may be characterized as a one step overall reaction (complete dehalogenation followed by pyrolysis of xanthine), with two sharp increases in the reaction rate, as evidenced by two peaks in the derivative thermogravimetric curve at 360 and 400°C.

Allopurinol (allo)

The thermal degradation of metal allopurinol complexes, (Fig. 4, Table 6) shows two principal processes. A dehydration reaction is followed by complete decomposition to the respective metal oxide. The decomposition of the dehydrated complexes occurs in several hardly resolved steps over a variable temperature range. In accordance with the data observed in the hypoxanthine compounds, the allopurinol complexes of cobalt, nickel and especially of copper show higher reaction rates for the pyrolyses than zinc and cadmium complexes. The dehydration of the metal complexes of the type $M(allo)_2SO_4 \cdot 4H_2O$ (M is Co, Ni, Zn, Cd) although exhibiting two different bonding types for the water molecules, occurs in a one step reaction. Under the experimental conditions used there was no evidence for the formation of stable compounds with intermediate degrees of hydration.

In contrast to the findings mentioned above, for the dehydration of the isostructural copper complex a separation in two steps could be deduced. The decrease in mass of 11.2% of the first step of the dehydration reaction is in agreement with the calculated value for three water molecules (10.7%). The second step with a mass loss of 3.3% corresponds to the release of the last water molecule. In view of the structure of the complex involving three coordinating and one noncoordinating water molecule, this two-step dehydration reaction could be interpreted as follows. The first step corresponds to the elimination of the noncoordinating water molecule and of the two more weakly bonded water molecules in the apical positions of the (4 + 2)-Jahn–Teller-distorted copper coordination octahedron. This would imply an intermediate structure in which copper exhibits a

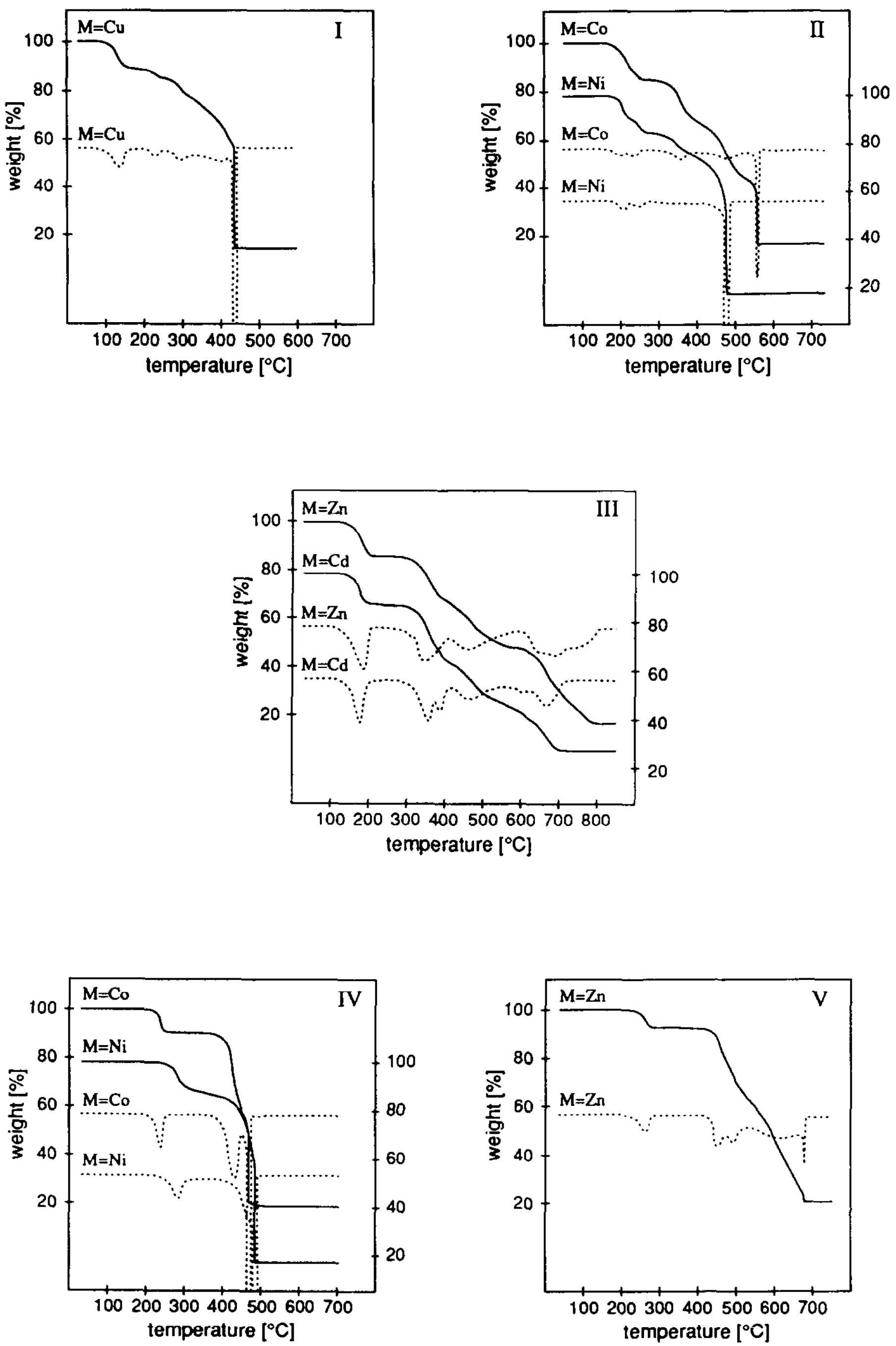

Fig. 4. Thermogravimetric (solid lines) and differential thermogravimetric (dotted lines) curves of the thermal degradation of metal allopurinol complexes in flowing oxygen atmosphere: I, M(allopurinol)$_2$SO$_4$ · 4H$_2$O (M is Cu); II, M(allopurinol)$_2$SO$_4$ · 4H$_2$O (M is Co, Ni); III, M(allopurinol)$_2$SO$_4$ · 4H$_2$O (M is Zn, Cd); IV, M(allopurinol)$_2$Cl$_2$ · 2H$_2$O (M is Co, Ni); V, Zn(allopurinol$^-$)Cl · H$_2$O.

TABLE 6

Thermal degradation [a] of metal allopurinol complexes

Complex	Dehydration			Total decomp.		Final product
	Mass loss/%		T/°C	Mass loss/%	T/°C	
$Cu(allo)_2SO_4 \cdot 4H_2O$	$-3H_2O$	10.7 (c)	80–180			
		11.2 (o)				
	$-1H_2O$	3.6 (c)	180–250	84.2 (c_{CuO})	250–440	CuO/Cu_2O
		3.3 (o)		85.6 (o)		
$Co(allo)_2SO_4 \cdot 4H_2O$	$-4H_2O$	14.4 (c)	150–250	83.9 (c)	280–560	Co_3O_4
		14.5 (o)		82.1 (o)		
$Ni(allo)_2SO_4 \cdot 4H_2O$	$-4H_2O$	14.4 (c)	160–270	85.0 (c)	270–480	NiO
		14.8 (o)		85.9 (o)		
$Zn(allo)_2SO_4 \cdot 4H_2O$	$-4H_2O$	14.2 (c)	120–210	83.9 (c)	250–800	ZnO
		14.2 (o)		83.2 (o)		
$Cd(allo)_2SO_4 \cdot 4H_2O$	$-4H_2O$	13.0 (c)	120–220		240–710	$CdO/Cd_3O_2SO_4$
		12.8 (o)		73.0 (o)		
$Co(allo)_2Cl_2 \cdot 2H_2O$	$-2H_2O$	8.2 (c)	200–250	81.7 (c)	320–470	Co_3O_4
		8.6 (o)		81.4 (o)		
$Ni(allo)_2Cl_2 \cdot 2H_2O$	$-2H_2O$	8.2 (c)	220–320	82.9 (c)	320–480	NiO
		11.5 (o)		83.1 (o)		
$Zn(allo^-)Cl \cdot H_2O$	$-1H_2O$	7.1 (c)	200–280	68.0 (c)	350–680	ZnO
		7.6 (o)		79.5 (o)		

[a] c, Calculated; o, observed.

square-planar coordination. The second step corresponds to the release of the remaining, firmly bonded, water molecule in the equatorial plane of the coordination octahedron. The complete decomposition of $Cu(allopurinol)_2SO_4$ to Cu_2O and CuO occurs with a sharp increase of the reaction rate at about 430°C.

In respect of these sulphato complexes, the start of the dehydration reaction of the chloro complexes $M(allo)_2Cl_2 \cdot 2H_2O$ (M is Co, Ni) is shifted towards higher temperatures. The removal of the two coordinating water molecules of the cobalt compound reveals a stable dehydrated intermediate phase. In contrast, in the nickel complex the dehydration is overlapping with the pyrolysis of the ligand, and therefore the observed mass loss of the first step is higher than that calculated for two water molecules.

The thermal decomposition of $Zn(allo^-)Cl \cdot H_2O$ finally takes place in a pronounced two step reaction. Dehydration, starting at a temperature of about 200°C, reveals an anhydrate phase, which is stable in the temperature range 280–350°C. The observed decrease in mass during the first decomposition step (7.6%) is in accord with the values calculated for the loss of one water molecule per formula unit (7.1%). The anhydrous zinc complex is decomposed to ZnO in the temperature range 350–680°C.

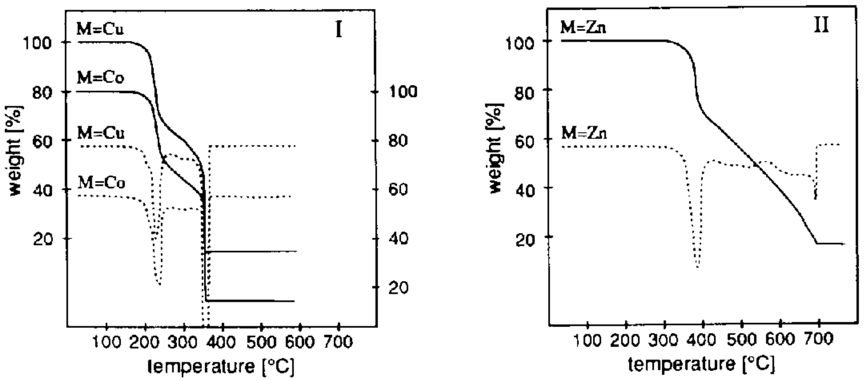

Fig. 5. Thermogravimetric (solid lines) and differential thermogravimetric (dotted lines) curves of the thermal degradation of metal alloxanthine complexes in flowing oxygen atmosphere: I, M(alloxanthine)$_2$(NO$_3$)$_2$ · 2H$_2$O (M is Cu, Co); II, Zn(alloxanthine)$_2$Cl$_2$.

Alloxanthine (alloxan)

The thermal degradation data are presented in Fig. 5 and Table 7. Complexes of the type M(alloxan)$_2$(NO$_3$)$_2$ · 2H$_2$O (M is Cu, Co) exhibit strikingly similar thermal decomposition behaviour, indicating their isostructural relationship. Both degradations occur in two well defined steps, the curve of the copper complex indicating a slightly higher reaction rate than the analogous cobalt compound. The mass losses of the first step correspond approximately to the simultaneous elimination of two water molecules and of two nitrate groups, probably in the form of HNO$_3$ molecules. The subsequent decomposition of the copper complex is finished at a temperature of 370°C (final products CuO and Cu$_2$O), whereas the

TABLE 7

Thermal degradation [a] of metal alloxanthine complexes

Complex	Dehydration		T/°C	Total decomp.		Final product
	Mass loss/%			Mass loss/%	T/°C	
Cu(alloxan)$_2$(NO$_3$)$_2$ · 2H$_2$O	−2H$_2$O −2HNO$_3$	6.8 (c) 23.9 (c) ~33 (o)	170–250	84.9 (c$_{CuO}$) 87.2 (o)	250–370	CuO/Cu$_2$O
Co(alloxan)$_2$(NO$_3$)$_2$ · 2H$_2$O	−2H$_2$O −2HNO$_3$	6.9 (c) 24.1 (c) ~29 (o)	170–260	84.7 (c$_{Co_3O_4}$) 86.7 (o)	260–370	Co$_3$O$_4$/CoO/Co
Zn(alloxan)$_2$Cl$_2$				81.5 (c) 84.6 (o)	290–720	ZnO

[a] c, Calculated; o, observed.

pyrolysis of the cobalt compound reveals Co_3O_4, CoO and Co as final products at a temperature of 370°C.

The anhydrous zinc complex $Zn(alloxan)_2Cl_2$ is decomposed to ZnO in a two step reaction without the formation of a stable intermediate.

Uric acid (hur)

The thermal degradation data are presented in Fig. 6 and Table 8. The pyrolytic decomposition of the dehydrated or desolvated compounds generally takes place in two hardly resolved steps, starting at temperatures between 230 and 390°C.

$Na(hydrogenurate^-) \cdot H_2O$ undergoes a three-step degradation reaction. In the first two steps the water of hydration is eliminated, resulting in a relatively unstable anhydrous phase.

The TG curve of $M(hur^-)$ (M is K, Rb) proves the anhydrous character of these compounds. A slightly reduced thermal stability of the hydrogenurate anion is observed with respect to the free ligand. The decomposition starts at about 335°C (K) and 280°C (Rb) respectively, whereas pure anhydrous uric acid is thermally stable up to 440°C under comparable experimental conditions [9].

The thermal degradation of $NH_4(hydrogenurate^-)$ takes place in two well distinguishable reaction steps: elimination of one NH_3 molecule followed by the decomposition of phase I uric acid formed as an intermediate.

The two phases of $Mg(hur^-)_2 \cdot 8H_2O$ exhibit very similar structures with $[Mg(H_2O)_6]^{2+}$ octahedra, non-coordinating hur-anions and two additional hydrogen-bonded water molecules. In accord with these structures, the two phases show a strikingly similar decomposition behaviour. Thermogravimetric measurement and differential scanning calorimetry data show that the dehydration of both phases occurs in two distinct steps with $Mg(hydrogenurate^-)_2 \cdot 6H_2O$ as an intermediate phase. The first dehydration step $(-2H_2O)$ is a topotactic reaction with three-dimensional preservation of the main structure elements of the octahydrate in the structure of the hexahydrate [12].

The thermal decomposition of the metal complexes of the type $M(hydrogenurate^-)_2 \cdot 6H_2O$ (M is Ca, Co, Cu) starts with a dehydration process which is followed by complete decomposition to the corresponding metal oxides in the case of the cobalt and copper complexes.

6-Mercaptopurine (MP)

The thermal degradation curves of the mercaptopurine complexes are shown in Fig. 7, whereas the respective analytical data are given in Table 9.

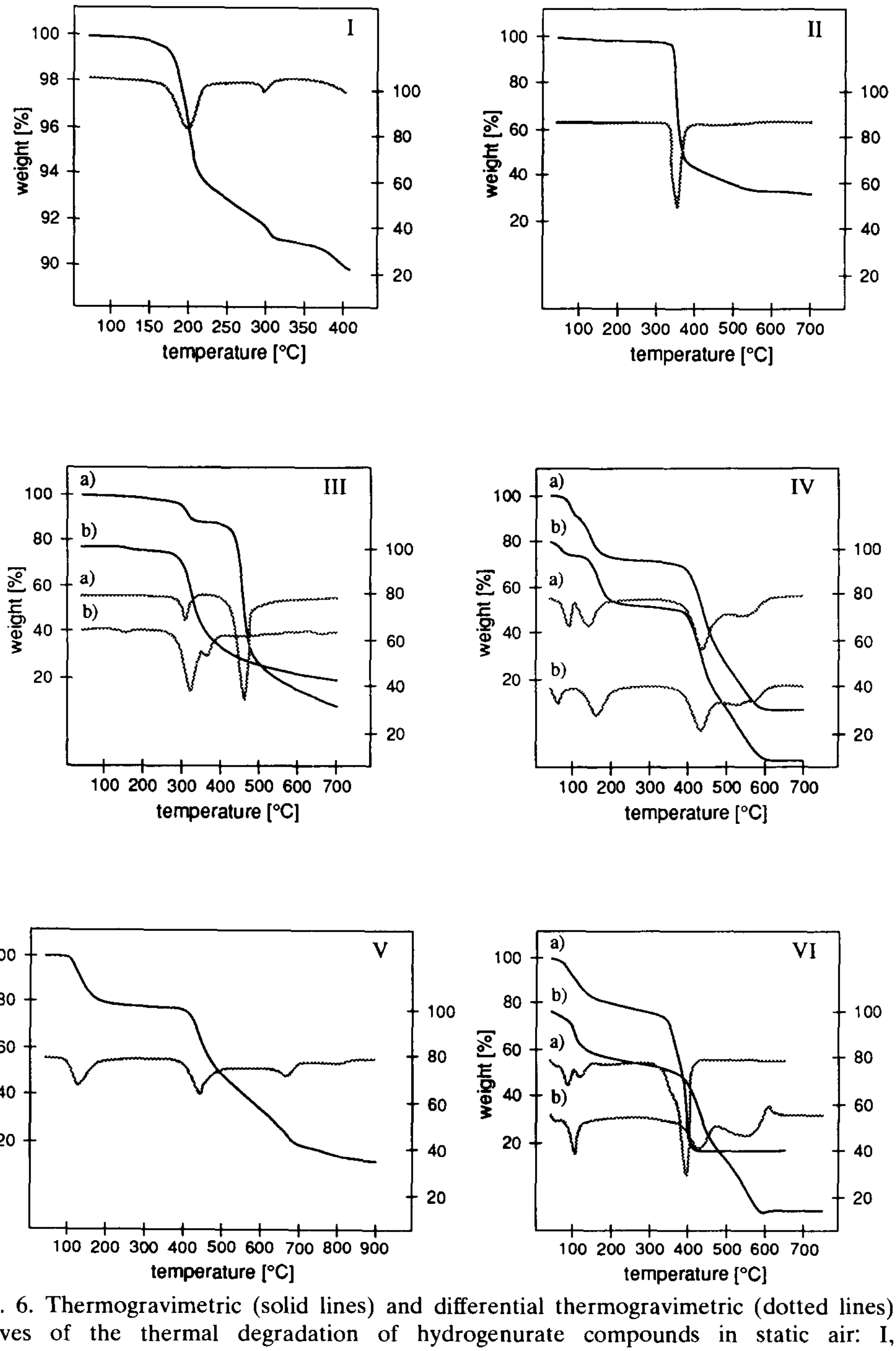

Fig. 6. Thermogravimetric (solid lines) and differential thermogravimetric (dotted lines) curves of the thermal degradation of hydrogenurate compounds in static air: I, Na(hydrogenurate$^-$) · H_2O; II, K(hydrogenurate$^-$), III, (a) NH_4(hydrogenurate$^-$), (b) Rb(hydrogenurate$^-$); IV, (a) Mg(hydrogenurate$^-$)$_2$ · $8H_2O$ (phase I), (b) Mg(hydrogenurate$^-$)$_2$ · $8H_2O$ (phase II); V, Ca(hydrogenurate$^-$)$_2$ · $6H_2O$; VI, (a) Co(hydrogenurate$^-$)$_2$ · $6H_2O$, (b) Cu(hydrogenurate$^-$)$_2$ · $6H_2O$.

TABLE 8

Thermal degradation [a] of metal hydrogenurate compounds

Compound	Desolvation			Start of decomposition T/°C
	Mass loss/%		T/°C	
$Na(hur^-) \cdot H_2O$	$-H_2O$	8.7 (c) 8.8 (o)	40–300	320
$NH_4(hur^-)$	$-NH_3$	9.2 (c) 11.2 (o)	140–320	390
$K(hur^-)$				335
$Rb(hur^-)$				280
$Mg(hur^-)_2 \cdot 8H_2O$ (I)	$-2H_2O$	7.2 (c) 6.1 (o)	50–105	350
	$-6H_2O$	21.5 (c) 20.2 (o)	105–270	
$Mg(hur^-)_2 \cdot 8H_2O$ (II)	$-2H_2O$	7.2 (c) 9.1 (o)	70–95	350
	$-6H_2O$	21.5 (c) 21.6 (o)	110–280	
$Ca(hur^-)_2 \cdot 6H_2O$	$-6H_2O$	22.4 (c) 21.4 (o)	80–290	355
$Co(hur^-)_2 \cdot 6H_2O$	$-6H_2O$	21.6 (c) 22.4 (o)	40–280	284 ($\rightarrow Co_3O_4$)
$Cu(hur^-)_2 \cdot 6H_2O$	$-6H_2O$	21.4 (c) 21.4 (o)	45–70	265 ($\rightarrow CuO$)

[a] c, Calculated; o, observed.

The thermogravimetric degradation curves of the monomeric complexes of the type $M(MP)_2Cl_2 \cdot CH_3OH$ (M is Mn, Co, Zn, Fe) show three reaction steps. The first mass loss corresponds to the elimination of methanol as evidenced by mass spectrometric investigations. The desolvated intermediate products are decomposed in two poorly resolved steps due to overlapping of total dehalogenation and pyrolyses of the organic moiety.

Complexes of the type $M(MP)_4Cl_2$ (M is Fe, Co) containing both coordinating and non-coordinating mercaptopurine molecules are stable up to 230°C (Co) or 420°C (Fe). The degradation of the cobalt compound reveals a relatively stable intermediate product of unknown stoichiometry at about 400°C.

The dehydration of the monomeric complex $Pt(MP^-)_2 \cdot 2H_2O$ occurs in the temperature range 100–180°C under formation of an anhydrous phase stable up to 425°C. The dehydration complex decomposes to metallic platinum. The start of the pyrolysis of the coordinating mercaptopurine anion is shifted towards higher temperatures (425°C) with respect to the dehydration of pure neutral mercaptopurine (300°C).

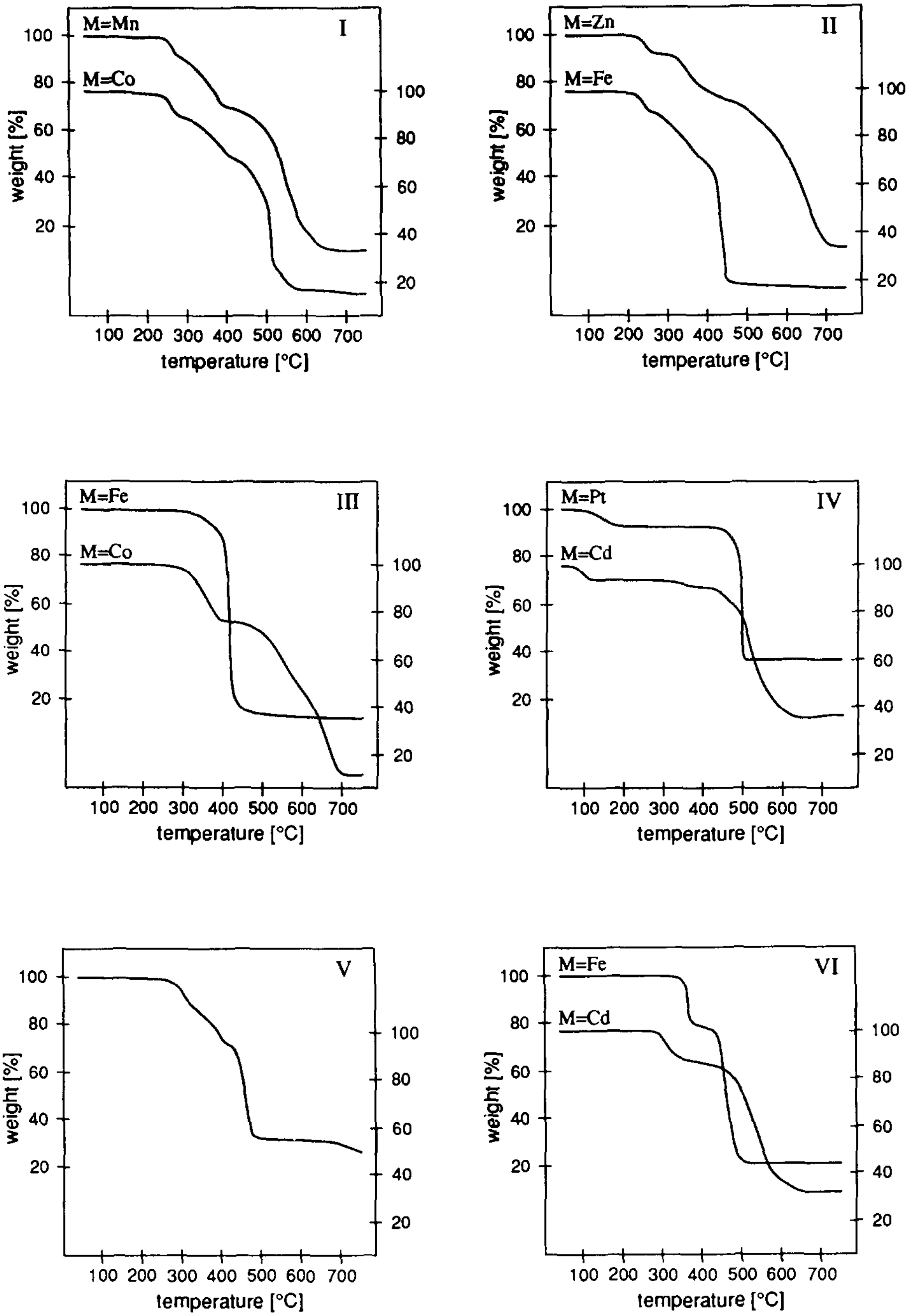

Fig. 7. Thermogravimetric curves of the thermal degradation of metal mercaptopurine complexes in static or flowing air (exception: Pt(mercaptopurine $)_2 \cdot 2H_2O$, flowing nitrogen atmosphere: I, M(mercaptopurine)$_2$Cl$_2 \cdot CH_3OH$ (M is Mn, Co); II, M(mercaptopurine)$_2$Cl$_2 \cdot CH_3OH$ (M is Zn, Fe); III, M(mercaptopurine)$_4$Cl$_2$ (M is Fe, Co); IV, M(mercaptotpurine$^-$)$_2 \cdot 2H_2O$ (M is Pt, Cd); V, Cu(mercaptopurine$^+$)Cl$_2$; VI, (Fe$_2$-(mercaptopurine)$_3$Cl$_5$ and Cd$_3$(mercaptopurine)$_4$Cl$_6$.

TABLE 9

Thermal degradation [a] of metal mercaptopurine complexes

Complex	Desolvation			Total decomp.		Final product
	Mass loss/%		T/°C	Mass loss/%	T/°C	
$Mn(MP)_2Cl_2 \cdot CH_3OH$	$-CH_3OH$	6.9 (c) 8.5 (o)	250–280	83.5 (c) 88.2 (o)	280–650	Mn_3O_4
$Co(MP)_2Cl_2 \cdot CH_3OH$	$-CH_3OH$	6.9 (c) 9.2 (o)	200–270	82.8 (c) 83.3 (o)	270–730	Co_3O_4
$Zn(MP)_2Cl_2 \cdot CH_3OH$	$-CH_3OH$	6.8 (c) 7.9 (o)	190–260	82.8 (c) 86.9 (o)	260–720	ZnO
$Fe(MP)_2Cl_2 \cdot CH_3OH$	$-CH_3OH$	6.9 (c) 8.4 (o)	190–250	82.8 (c) 82.9 (o)	250–670	Fe_2O_3
$Fe(MP)_4Cl_2$				89.1 (c) 88.7 (o)	420–460	Fe_2O_3
$Co(MP)_4Cl_2$				89.1 (c) 89.1 (o)	230–710	Co_3O_4
$Pt(MP^-)_2 \cdot 2H_2O$	$-2H_2O$	6.8 (c) 7.7 (o)	100–180	63.4 (c) 63.6 (o)	425–500	Pt
$Cd(MP^-)_2 \cdot 2H_2O$	$-2H_2O$	9.9 (c) 7.1 (o)	60–120	64.6 (c_{CdO}) 65.2 (o)	305–750	$CdO/Cd_3O_2SO_4$ β-$CdSO_4$
$Fe_2(MP)_3Cl_5$	$-HCl$	4.9 (c) 4.4 (o)	250–355	78.6 (c) 79.6 (o)	355–510	Fe_2O_3
$Cu(MP^+)Cl_2$				72.3 (c) 73.2 (o)	235–810	CuO
$Cd_3(MP)_4Cl_6$				66.8 (c_{CdO}) 69.6 (o)	250–660	$CdO/Cd_3O_2SO_4$

[a] c, Calculated; o, observed.

The polymeric complex $Cd(MP^-)_2 \cdot 2H_2O$ exhibits a first step with a mass loss attributed to the elimination of two water molecules per formula unit. The decomposition of the anhydrous compound starts at 350°C and results in the formation of $Cd_3O_2SO_4$ and minor amounts of β-$CdSO_4$ and CdO. The structure of $Fe_2(MP)_3Cl_5$ consists of $[Fe^{II}(MP)_3]^{2+}$ cations, $[Fe^{III}Cl_4]^-$ anions and free Cl^- ions [8]. Its thermal degradation occurs in several overlapping steps. The first decrease in mass observed in the temperature range 250–355°C probably refers to the elimination of a HCl molecule involving the non-coordinating chloride ion. The intermediate formed is finally decomposed to Fe_2O_3.

The anhydrous complex $Cu(MP^+)Cl_2$ representing a dimeric structure with bridging chloride ions [13], is stable up to 235°C. The subsequent decomposition results in CuO, due to simultaneous dehalogenation and pyrolysis processes.

The anhydrous complex $Cd_3(MP)_4Cl_6$ is finally decomposed in a two-step reaction to the final residues $Cd_3O_2SO_4$ and CdO.

REFERENCES

1 E.J. Stiefel, Progr. Inorg. Chem., 22 (1977) 1.
2 R. Hille and V. Massey, Nucleic acid–metal interactions, in T.G. Spiro (Ed.), Metals Ions in Biology, Vol. 7, Wiley, New York, 1985, p. 443.
3 T.R. Hawkes, G.N. George and R.C. Bray, Biochem. J., 218 (1984) 961.
4 K. Jewers, in E. Jucker (Ed.), Progress in Drug Research, Vol. 25, Birkhäuser, Basel, Switzerland, 1981, p. 275.
5 G.B. Elion, Angew. Chem., 101 (1989) 893.
6 S. Kischner, Y.K. Wei, D. Francies and J.G. Bergman, J. Med. Chem., 9 (1969) 369.
7 G. Hänggi, Ph.D. Dissertation, University of Zürich, Switzerland, 1992.
8 E. Gyr, Ph.D. Dissertation, University of Zürich, Switzerland, 1991.
9 Z. Kopajtic, Ph.D. Dissertation, University of Zürich, Switzerland, 1985.
10 Powder Diffraction File, JCPDS, Swarthmore, PA, USA, Cards No. 35-609, 5-661, 5-667, 9-402, 9-418, 15-806, 4-835, 36-1451, 5-640, 32-140, 4-0802, 15-85.
11 E. Colacio-Rodriguez, J.D. López-González and J.M. Salas-Peregrin, J. Therm. Anal., 28 (1983) 3.
12 E. Dubler, G. Jamson and Z. Kopajtic, J. Inorg. Biochem., 26 (1986) 1.
13 E. Dubler and E. Gyr, Inorg. Chem., 27 (1988) 1466.
14 E. Dubler, G. Hänggi and W. Bensch, J. Inorg. Biochem., 29 (1987) 269.
15 E. Dubler, G. Hänggi and H. Schmalle, Acta Crystallogr., Sect. C, 43 (1987) 1872.
16 E. Dubler, G. Hänggi and H. Schmalle, Inorg. Chem., 29 (1990) 2518.
17 G. Hänggi, H. Schmalle and E. Dubler, Acta Crystallogr., Sect. C, 48 (1992) 1008.
18 E. Dubler, G. Hänggi and H. Schmalle, Inorg. Chem., 31 (1992) 3728.
19 G. Hänggi, H. Schmalle and E. Dubler, Inorg. Chim. Acta, 197 (1992) 135.
20 G. Hänggi, H. Schmalle and E. Dubler, Acta Crystallogr., Sect. C, 47 (1991) 1609.
21 G. Hänggi, H. Schmalle and E. Dubler, Inorg. Chem., 27 (1988) 3131.
22 G. Hänggi, H. Schmalle and E. Dubler, Acta Crystallogr., Sect. C, 44 (1988) 1560.
23 G. Hänggi, H. Schmalle and E. Dubler, J. Chem. Soc. Dalton Trans., (1993) 941.
24 G. Hänggi, H. Schmalle and E. Dubler, Inorg. Chem., in press.